Powder Technology 342 (2019) 11–23

Contents lists available at ScienceDirect

Powder Technology

journal homepage: www.elsevier.com/locate/powtec

Densification, microstructure evolution and fatigue behavior of Ti-13Nb-13Zr alloy processed by selective laser melting

Libo Zhou [a], Tiechui Yuan [a,*], Ruidi Li [a,*], Jianzhong Tang [b], Guohua Wang [b], Kaixuan Guo [b], Jiwei Yuan [c]

[a] State Key Laboratory of Powder Metallurgy, Central South University, Changsha 410083, PR China
[b] Zhuzhou Printing Additive Manufacturing Co. LTD, Zhuzhou 412000, PR China
[c] Guizhou R&D Center of Titanium Materials Co. LTD, Zunyi 563004, PR China

ARTICLE INFO

Article history:
Received 23 January 2018
Received in revised form 6 September 2018
Accepted 24 September 2018
Available online 26 September 2018

Keywords:
Selective laser melting
Ti-13Nb-13Zr
Densification
Microstructural
Fatigue behavior

ABSTRACT

Ti-13Nb-13Zr alloy was fabricated by selective laser melting (SLM), and the densification, microstructure evolution, nanohardness, tensile strength and fatigue behavior of the alloy were systematically investigated. A narrow, feasible process window (laser power 325 W, scanning speed 1000 mm/s, scanning distance 0.13 mm, and layer thickness 0.03 mm) was accordingly determined. With the increase of scanning speed, the coarse acicular-shaped α′ grains changed to refined acicular-shaped α′ grains and then defect formed in the microstructure. The optimally prepared Ti-13Nb-13Zr sample had a very high hardness of 519.448 HV and tensile strength of 1106.07 MPa, which are superior higher than that prepared by traditional thermomechanical technique (280 ± 15 HV and 732 MPa). Owing to the change of BCC to HCP structure ([111] β→ [1-21-3] α′), the accumulation of dislocations and the finer grains, the SLM-processed samples exhibited higher fatigue strength than that the alloy processed by cast and was commensurate with the cast Ti-6Al-4 V. Moreover, the influences of phase transition on fatigue behavior have been discussed carefully.

1. Introduction

Titanium and its alloys are widely used in medical applications because of their unique properties, such as corrosion resistance [1], mechanical strength [2,3] and superior biocompatibility [4–6]. Ti-6Al-4 V alloy was the first Ti alloy used as biomaterial which was originally developed for aerospace applications [7]. However, in recent years, there has been a lot of negative comments about vanadium ion and aluminum ion on causing health problems like cytotoxic effects, adverse tissue reaction and neurological disorders [5,7]. Moreover, the mismatch of elastic modulus between Ti-6Al-4 V (120 GPa) and human bone (30 GPa) could lead to a resorption of the adjacent bone tissue [4,5]. The elastic modulus of Ti-13Nb-13Zr (65 GPa), compared with the elastic modulus of Ti-6Al-4 V (120 GPa), is closer to that of human bone [8]. Consequently, the stress-shielding effects and mismatch problem are reduced. What's more, all the three constituents in the Ti-13Nb-13Zr alloy meet the criterial for biomaterials in terms of biocompatibility, mechanical consideration, resistance to corrosion, and ionic cytotoxicity [9,10]. Therefore, in recent years, Ti-13Nb-13Zr alloy has attracted a growing number of researchers.

Most of works reported on the process of Ti-13Nb-13Zr alloy are focused on the severe plastic deformation (SPD) or arc melting. Baptista et al. [11] studied the fatigue behavior of arc melted Ti-13Nb-13Zr alloy and the result turns out that Ti-13Nb-13Zr shows high fatigue resistance when compared with the CP Ti and annealed Ti-6Al-4 V. Lee et al. [12] researched the microstructure tailoring of Ti-13Nb-13Zr to enhance the strength and ductility for biomedical applications. Urbańczyk et al. [13] demonstrated that the corrosion resistance of Ti-13Nb-13Zr alloy could be improved through the plasma electrolytic oxidation (PEO) process. Geetha et al. [14] revealed that the even distribution of alloying elements in Ti-13Nb-13Zr alloy bring superior corrosion resistance. Bobbili et al. [15] investigated the dynamic recrystallization behavior of Ti-13Nb-13Zr and found that increasing the deformation temperature and decreasing the strain rate can promote the process of dynamic recrystallization. Ivana et al. [16] investigated the metallic ion release of ultrafine-grained Ti-13Nb-13Zr alloy processed by high pressure torsion (HPT) and they found that the number of released ions of the Ti-13Nb-13Zr alloy processed by HPT was higher than that produced by traditional casting. Suresh et al. [17,18] researched the equal channel angular extrusion (ECAE) of the Ti-13Nb-13Zr alloy and confirmed that corrosion resistance of the ultrafine-grained alloys obtained by ECAE was higher than the non-treated material. All of the forming methods discussed above can only process standard implants. However, as a biocompatible metal, Ti-13Nb-13Zr can be processed into the complex shapes of functional implants is very important.

Among different possible methods to manufacture complex construction, selective laser melting is a specifically versatile and advantageous

* Corresponding authors.
E-mail addresses: tiechuiyuan@csu.edu.cn (T. Yuan), liruidi@csu.edu.cn (R. Li).

https://doi.org/10.1016/j.powtec.2018.09.073
0032-5910/

way [19]. Using a laser to melt and solidify the required geometry layer-by-layer, SLM is able to produce intricate construction from metal powder materials [20]. SLM possesses a number of advantages over conventional manufacturing techniques, such as high material utilization rate, direct production based on the no geometric constraints mode [21,22]. The studies about SLM processed titanium and its alloys have attracted much attention [23,24]. Nevertheless, to the best knowledge of the authors, there are still no comprehensive previous studies focused on the fatigue behaviors of SLM processed sample, which are very important for biomedical materials.

In this study, in order to fully illuminate the fatigue behaviors of SLM processed sample, the densification, microstructure and mechanical properties in terms of hardness, tensile strength and fatigue behavior, various parameters of SLM processing Ti-13Nb-13Zr were investigated.

2. Experimental procedures

The powder was gas atomized from a Ti-13Nb-13Zr ingot and had a chemical composition as listed in Table 1. The differences between the analyzed composition of alloying elements and the nominal composition are very small, <0.4% for Nb, and 0.2% for Zr, respectively. The oxygen and nitrogen concentrations were too low to influence the alloy performance. The powder is spherical (Fig. 1(a)) and its particle size distribution is also shown in the figure as an inset.

All the samples were fabricated using a SLM apparatus (FS271M Farsoon, Inc., China) under a high-purity Ar atmosphere. The machine was equipped with a 480 W Yb:YAG fiber laser, which had a spot size of 80 μm. Cubes (10 mm × 10 mm × 10 mm) and standard tensile and fatigue samples were fabricated using a laser power (P) from 175 to 375 W and a scanning speed (v) from 800 to 1200 mm/s. The layer thickness (d) and scanning distance (h) were kept constant at 30 μm and 130 μm, respectively. The Eq. (1) [25]

$$E = P/vhd \tag{1}$$

was used to evaluate the laser energy that input to the powder layer during process. Each layer was alternated by 60° and scanned using a continuous laser mode shown in Fig. 1(b).

Table 1
Analyzed chemical compositions of Ti-13Nb-13Zr alloy (mass fraction, %).

Element	Ti	Nb	Zr	O	N
Content	Balance	12.66	13.12	0.038	0.013

The Archimedes' method was applied to measure the density of specimens. Phase analysis was performed by X-ray diffraction (XRD, Rigaku D/MAX-2250) with a Cu K_α radiation. Metallographic samples were etched by the Kroll's reagent, which were prepared according to the standard procedures. The optical microscope (Germany Leica), a FEI Quanta FEG 250 filed emission gun scanning electron microscope (FEG-SEM) and a JEOL 2100F transmission electron microscope (TEM) were used to observe the microstructures of the samples. The samples for TEM observation were prepared under the following conditions: electrolytic polishing with a mixture of 60% methanol, 34% normal butanol and 6%perchloric acid at 243 K in temperature and 23 V in voltage.

Four samples were prepared for tensile tests under each condition using an Instron 3369 machine with a crosshead speed of 1 mm/min. A loading–unloading test mode was used with a force of 30 mN and holding time of 10 s. The recorded load and indentation depth data were used to build the loading–unloading plots. The indentations were verified by atomic force microscope (America Veeco AFM). The fatigue behavior was tested under the condition of 20 Hz with a stress ratio $R = 0.1$ according to DIN 50113. The samples were cycled with constant stress amplitude until failure and the S—N curves were plotted. The initial load was set at a maximum level estimated at about 80% yield strength (YS). To investigate the details and the mode of fracture, the fatigue fractography observations were performed using SEM. The tensile direction of the specimens in the tensile and fatigue tests in this work is in the scanning direction.

3. Results

3.1. Optimisation of processing parameters

The SLM processing parameters highly affect the quality of products. In this work, the laser power and the scanning speed were systematically varied. The parameters were set as follows: laser power 175–375 W; scanning speed 800–1200 mm/s; fixed layer distance 0.03 mm and scanning distance 0.13 mm. Fig. 2(a) indicates this parameter window mainly covers the low energy density ($E < 70$ J/mm^3), medium energy density (70 J/mm^3 < E < 90 J/mm^3) and high energy density ($E > 90$ J/mm^3). Fig. 2(b) shows the typical surface morphologies of the SLM-processed Ti-13Nb-13Zr samples including three regimes at a relatively low magnification. In the SLM process, laser scanning was performed line by line and the laser energy melt a row of powder particles and formed a continuous liquid track in cylindrical shape [25]. The surfaces of Ti-13Nb-13Zr samples processed by SLM show no apparent pores and cracks for all tests. At relatively low energy density (Area I in Fig. 2(a)), several clusters of micro-sized balls were formed on the surface which increased the roughness of the product significantly. The liquid solidification front became considerably disordered which results in the formation of interrupted scan tracks and the formation

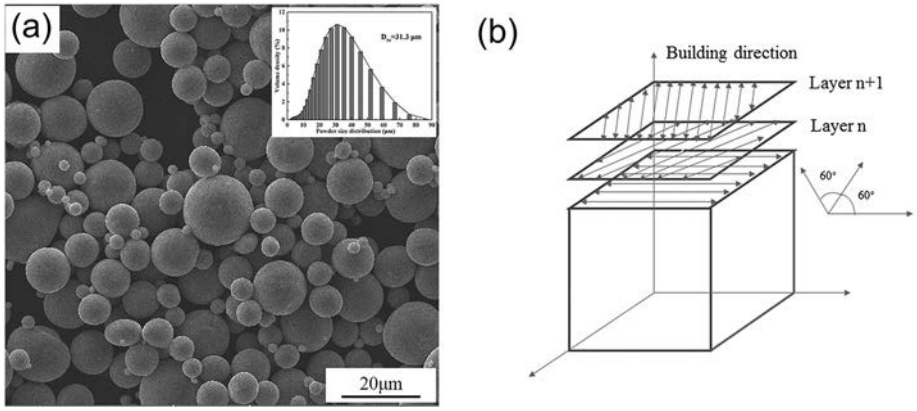

Fig. 1. (a) The morphology and particle size distribution of the starting Ti-13Nb-13Zr powder, (b) Schematic diagram of scanning mode.